Food Research International 182 (2024) 114142

Contents lists available at ScienceDirect

Food Research International

journal homepage: www.elsevier.com/locate/foodres

Innovative vs classical methods for drying heterotrophic *Chlorella vulgaris*: Impact on protein quality and sensory properties

Simon Van De Walle [a,b,*], Imma Gifuni [c], Bert Coleman [a], Marie-Christin Baune [d], Alexandre Rodrigues [e], Helena Cardoso [f], Fabio Fanari [g], Koenraad Muylaert [b], Geert Van Royen [a]

[a] Flanders Research Institute for Agriculture, Fisheries and Food (ILVO), Technology and Food Science Unit, Brusselsesteenweg 370, 9090 Melle, Belgium
[b] Biology Department KULAK, KU Leuven Kulak, Etienne Sabbelaan 53, 8500 Kortrijk, Belgium
[c] AlgoSource Technologies SAS, 7 Rue Eugène Cornet, 44600 Saint-Nazaire, France
[d] German Institute of Food Technologies (DIL e.V.), Prof.-von-Klitzing-Str. 7, 49610 Quakenbrück, Germany
[e] Necton S.A., Belamandil s/n., 8700-152 Olhao, Portugal
[f] Allmicroalgae Natural Products S.A., 2445-413 Pataias, Portugal
[g] Food Industries, Institute of Agriculture and Food Research and Technology (IRTA), Finca Camps i Armet s/n, 17121 Monells, Spain

ARTICLE INFO

Keywords:
Microalgae
Drying
Functional properties
Digestibility
Sensory evaluation
Volatiles

ABSTRACT

Drying is a necessary step in the microalgae production chain to reduce microbial load and oxidative degradation of the end product. Depending on the differences in applied temperature and treatment time, the process of drying can have a substantial impact on protein quality and aroma, important characteristics determining the incorporation potential in food products. In this study, we compared the drying of heterotrophic *Chorella vulgaris* with both innovative (agitated thin film drying (ATFD), pulse combustion drying (PCD) and solar drying (SolD)) and commonly used drying techniques (spray drying (SprD) and freeze drying (FD)). To evaluate the impact on protein quality, we evaluated techno-functional properties, *in vitro* digestibility (INFOGEST) as well as protein denaturation using differential scanning calorimetry (DSC). A sensory analysis was performed by a trained expert panel, combined with headspace solid-phase microextraction (HS-SPME) - gas chromatography-mass spectrometry (GC–MS) to determine volatile organic compounds (VOCs). ATFD was found to increase techno-functional properties such as gelling, water holding and solubility as well as *in vitro* protein digestibility. These observations could be related to induced cell disruption and protein denaturation by ATFD. Sensory analysis indicated an increased earthy off-flavor after ATFD. Interestingly, the high-temperature PCD led to an increase in cacao odor while low-temperature FD resulted in lower flavor, odors and VOCs. These results demonstrate that protein quality and sensorial properties of *C. vulgaris* can be steered through the type of drying, which could help in the selection of application-specific drying methods. Overall, this work could promote the incorporation of microalgal single cell proteins in different innovative food products.

1. Introduction

Due to increasing concerns over animal production for meat, a transition is taking place from animal-based to plant-based protein foods. This trend has pushed research efforts to consider alternative high-quality sources of protein such as unicellular organisms, especially for functional proteins. In this respect, microalgae received significant interest lately as a promising functional protein ingredient in foods (Acquah, Ekezie, & Udenigwe, 2021). The genus *Chlorella* is one of the most frequently consumed microalgal species, and has been commercially cultivated since the 1960s (Demarco, Oliveira de Moraes, Matos, Derner, de Farias Neves, & Tribuzi, 2022). The default growth condition of *C. vulgaris* is photoautotrophy (light as an energy source). However, it is also able to grow heterotrophically on various organic carbon sources.

Abbreviations: ATFD, Agitated thin film drying; SprD, spray drying; FD, freeze drying; PCD, pulse combustion drying; SolD, solar drying; DSC, differential scanning calorimetry; HS-SPME, headspace solid-phase microextraction; GC-MC, gas chromatography-mass spectrometry; a_w, water activity; dry weight, DW; VOC, volatile organic compound; DH, degree of protein hydrolysis; N-solubility, nitrogen solubility; ECSG-ILVO, Ethical Standards of the Commission of Flavor and Odor of ILVO; PCA, principal component analysis; OAV, odor activity value; ΔH, denaturation enthalpy; T_d, denaturation temperature.

* Corresponding author.
E-mail address: simon.vandewalle@ilvo.vlaanderen.be (S. Van De Walle).

https://doi.org/10.1016/j.foodres.2024.114142
Received 20 December 2023; Received in revised form 9 February 2024; Accepted 17 February 2024
Available online 18 February 2024

This heterotrophic growth condition is frequently used for large scale production because of the higher biomass concentration that can be achieved (over 100 g/L), lower operating costs, fewer contaminations and longer continuous operation (Barros et al., 2019; Kim, Park, Lee, Seon, Suh, Moon, & Chang, 2019; Klamczynska & Mooney, 2017). After the cultivation step, the biomass is usually dried in order to extend shelf life. Depending on the drying conditions, the colloidal properties of heat-sensitive compounds such as proteins could be impacted, resulting in altered protein quality (Brodkorb, Croguennec, Bouhallab, & Kehoe, 2016; de Farias Neves, Demarco, & Tribuzi, 2020). Moreover, *Chlorella* produces a range of volatile organic compounds (VOCs) that result in pronounced flavor profiles. Processing, and especially heat treatment, can cause degradation of existing and formation of new VOCs, resulting in a changed sensory profile (Coleman et al., 2023). Assessing the effect of the drying process is therefore fundamental for increasing the application of microalgae functional ingredients in innovative foods.

Drying is an important step in the microalgal production chain as this increases shelf life by minimizing microbial growth and oxidative deterioration (Stramarkou, Papadaki, Kyriakopoulou, & Krokida, 2017). Following cultivation, microalgal biomass is dewatered using flocculation, sedimentation, centrifugation or membrane filtration, resulting in a "wet paste" with 10–30 % DW (Chen, Chang, & Lee, 2015; de Farias Neves et al., 2020). This paste can be dried using various drying techniques which differ in applied temperature, exposure time and applied mechanical forces. Spray drying (SprD) is often applied for liquid foodstuffs (such as milk, coffee, …) and is also the preferred method for drying microalgal biomass (de Farias Neves et al., 2020). This technique typically results in a high quality and stable product as a result of the short exposure to high temperature (Chen et al., 2015; Show, Lee, Tay, Lee, & Chang, 2015; Zhang et al., 2022). Alternatively, freeze-drying (FD) is considered the most gentle drying method that favors preservation of heat-sensitive compounds (e.g. proteins, pigments, vitamins) because of the application of low temperatures and vacuum drying (Stramarkou et al., 2017). FD is also considered expensive because of the long operation time and only batch operation. Innovative drying techniques could provide similar or even improved protein quality with lower energy consumption. A recent study on solar drying (SolD) reported satisfactory protein quality of *Nannochloropsis oceanica* and *Tetraselmis chui* using solar thermal energy to reduce energy needs, although protein quality was slightly reduced compared to FD (Schmid et al., 2022). A main advantage of the SolD in this study is that it could theoretically operate completely off-grid using photovoltaic panels. Pulse combustion drying (PCD) utilizes principles similar to those of spray drying for product atomization. However, PCD uses direct combustion of a fossil fuel instead of resistive heating (electricity) to create a hot air current, resulting in better energetic efficiency during drying (Samborska et al., 2022). Higher temperature and shorter exposure time are applied during PCD (700–800 °C, milliseconds) compared to SprD (150–220 °C, seconds), which might impact protein quality (Samborska et al., 2022). Because of the low exposure time, the product only reaches a fraction of these temperatures during drying (Samborska et al., 2022). Agitated thin film drying (ATFD), which uses principles similar to thin layer drying, has been proposed as a mild drying technique for products that contain heat-sensitive compounds. This technique could also be used for viscous liquids that are difficult to dry, and is associated with relatively low energy input and operating costs (Acar, Dincer, & Mujumdar, 2022; Qiu, Boom, & Schutyser, 2019). These features of ATFD could make this type of dryer suitable for microalgae biomass with high solids content, while reducing energy usage. Although lower drying temperatures and longer exposure time are used in ATFD (60–100 °C, several minutes) compared to the other thermal drying methods, the shear forces generated by a rotating blade could potentially impact the microalgal cell wall and protein quality (Qiu et al., 2019). It is worth noting that most of the literature regarding the drying of microalgae is focused on non-food applications, while research related to food applications is limited (de Farias Neves et al., 2020).

Recent studies have demonstrated that microalgal proteins exhibit promising techno-functional properties. The diverse proteome of microalgae can facilitate interfacial stabilization at a broader pH and salt concentration range compared to conventional food proteins such as animal-derived proteins and soy (Acquah et al., 2021; Bertsch, Böcker, Mathys, & Fischer, 2021). Several studies have shown promising functional properties of proteins derived from various *Chlorella* species, especially exhibiting competitive emulsifying behavior compared to whey protein (Dai, Cepeda, Hinrichs, & Weiss, 2021; Ebert, Grossmann, Hinrichs, & Weiss, 2019; Grossmann, Ebert, Rg Hinrichs, & Weiss, 2019). *Chlorella* cells are characterized by a tough cell wall that limits solubilization of intracellular proteins, which is essential for protein molecular interactions and protein functionality in foods (Guil-Guerrero, Navarro-Juárez, López-Martínez, Campra-Madrid, & Rebolloso-Fuentes, 2004). The cell wall barrier can also restrict access of digestive enzymes to intracellular protein, which in turn reduces protein digestibility (Geada, Moreira, Silva, Nunes, Madureira, Rocha, Pereira, Vicente, & Teixeira, 2021). Nonetheless, some studies state that microalgal protein bioavailability and digestibility can be improved by disrupting the cell wall (Batista et al., 2020; Teuling, Schrama, Gruppen, & Wierenga, 2017; Van De Walle, Broucke, Baune, Terjung, Van Royen, & Boukid, 2023). Microalgae produce several VOCs which are responsible for their pronounced flavor (Coleman et al., 2022). Assessing the sensorial properties of protein rich microalgae are crucial for the food industry in order to incorporate this biomass in food and develop innovative and sustainable food products. To the best of our knowledge, the impact of drying on heterotrophic *Chlorella vulgaris* techno-functional properties, digestibility and sensory properties has so far not been investigated.

In this study, we aimed to compare the impact of five different drying techniques on the protein techno-functional properties and protein digestibility of heterotrophically cultivated *C. vulgaris*. The drying techniques include the most commonly used SprD and FD, as well as innovative techniques such as PCD, ATFD and SolD. Techno-functional properties included emulsifying, gelling, foaming, water/oil holding properties as well as solubility. *In vitro* protein digestibility was determined using the INFOGEST (Brodkorb et al., 2019) harmonized method followed by quantification of free amino groups and soluble nitrogen. Furthermore, other quality indicators such as protein denaturation and particle size were assessed. Additionally, the effect of drying method on the sensory properties of *C. vulgaris* was determined by a sensory evaluation using a trained taste panel and by the determination of the VOCs using headspace solid-phase microextraction (HS-SPME) coupled with gas chromatography-mass spectrometry (GC–MS). Finally, the nutritional composition of the dried *C. vulgaris* powders was assessed. As a comparison, reference protein isolates (soy, egg white) were included in the analyses to demonstrate the potential of the dried *Chlorella vulgaris* powders as a functional protein source.

2. Materials and methods

2.1. Biomass production

Heterotrophically cultivated *Chlorella vulgaris* frozen biomass was kindly supplied by Allmicroalgae Natural products S.A. (Pataias, Portugal). Heterotrophic *Chlorella vulgaris* was produced as previously reported by Schüler et al. (2020) starting in small Erlenmeyer flasks and scaled up sequentially until 200 L and 5000 L fermenters, according to standard commercial production (Schüler et al., 2020). Temperature was set to 30 °C and pH to 6.5 by the addition of ammonia solution (24 % w/w). The air inlet flowrate was adjusted to maintain approximately 1 L of air/L culture media/min, with agitation rate ranging between 100 and 1200 rpm to maintain sufficient dissolved oxygen in the medium. Heterotrophic medium (Barros et al., 2019), consisting of Guillard's F2 culture medium with added glucose (C:N ratio of 6.7:1), was used in the different scale-up stages and glucose was added in fed-batch to the 5 L,

200 L and 5000 L fermenters to keep a concentration between 1 and 20 g/L, while in the Erlenmeyer flasks there was only an initial addition of 20 g/L of glucose to the medium. Throughout the growing period, samples were collected aseptically twice a day to analyze the growth parameters. The biomass was harvested by centrifugation, and the wet paste (160 g/L DW) was packed in 10 or 20 L plastic containers and immediately frozen at −20 °C until drying.

Commercial spray dried soy protein isolate (SI) and egg white protein isolate (EWI) references (>80 % w/w protein) were kindly supplied by Solina Belgium S.A. (Nazareth, Belgium).

2.2. Drying techniques

The drying experiments conducted in this study include freeze drying (FD), spray drying (SprD), agitated thin film drying (ATFD), pulse combustion drying (PCD) and solar drying (SolD). The aim throughout these drying experiments was to obtain powders with a moisture content below 10 % and a water activity (a_w) below 0.60–0.65 to avoid microbial growth (Vera Zambrano, Dutta, Mercer, MacLean, & Touchie, 2019). Due to the utilization of pilot-scale equipment for drying the biomass and limited biomass availability, only a single drying trial was conducted for each method. A single homogenized batch of heterotrophic *C. vulgaris* was used, distributed to each of the drying locations.

2.2.1. Freeze drying

Freeze drying of the biomass (160 g/L DW)was performed at Necton (Olhao, Portugal) by sublimation in a freeze dryer F-50 (Frozen In Time Ltd, York, UK) with an ice condenser temperature of −50 °C. The dryer was equipped with six temperature probes to monitor the biomass temperature. The shelf temperature was first lowered to −30 °C and at pressure of 1000 mbar. Pressure was then lowered to 0.9 mbar at a constant shelf temperature of −30 °C. Finally, temperature was gradually increased to 30 °C in a timeframe of approximately 30 h.

2.2.2. Spray drying

Spray drying of the biomass (90 g/L DW, diluted with water) was performed at Allmicroalgae (Pataias, Portugal) using atomization in radial direction, facilitated by a rotating disc at 18,000 rpm. The biomass droplets were formed at the top of the drying tower with a volume of 40 m^3. The drying was performed with an air current temperature set at 200 °C, with the biomass exposure to the hot air current estimated in the order of several seconds. The heating of the air temperature was achieved by electric heating resistor modules (240 kW). At the bottom of the drying tower, the biomass powder was discharged with the outlet air temperature at 92 ± 3 °C. Powder and air were separated through a cyclone. Biomass exposure to the hot air is currently estimated to be in the order of several seconds.

2.2.3. Agitated thin film drying

Agitated thin film drying of the biomass (160 g/L DW, thawed) was performed at Bodec (Helmond, The Netherlands) with a tailor-made pilot scale thin film dryer by Technoforce Europe (Geleen, NL). The biomass was supplied at the top of the equipment using an electrical pump at a rate of 7.5 kg/h. Subsequently, the product was moved along the inner jacket using a rotating screw system at 800 rpm, creating a thin film with a thickness of 5 mm. The inner jacket was kept at a constant temperature of 98 °C and under a constant vacuum with a pressure of 30 mbar. The temperature of the product in the inner jacket is expected to be 5–10 °C lower than the inner jacket walls. After a residence time of 10 min in the jacket, powder was discharged at the bottom of the equipment in a plastic bag.

2.2.4. Pulse combustion drying

Pulse combustion drying of the biomass (160 g/L DW, thawed) was performed using a pilot model Ekonek PCD – 70 (Ekonek, Spain) at IRTA (Monells, Spain) with an evaporation capacity of 70 kg/h. The biomass was atomized by using compressed air (3 bar) and the internal pressure wave generated in the combustion motor at 130 Hz. The product was injected at a rate of 65 L/h with a pressure of 600 mbar. Although input air temperature could not be measured, air temperature was estimated at 600–800 °C. Drying was achieved with an outlet air temperature of 85 ± 1 °C at the exit of the primary. The total air flow coming out from the drier was 160 m^3/h with a temperature of 76 °C. The product was separated from the air and collected at the end of the cyclone separator. Biomass exposure to the hot air is currently estimated to be in the order of milliseconds.

2.2.5. Solar drying

Solar drying of the biomass (160 g/L DW, thawed) was performed at Necton (Olhao, Portugal), by convective drying in a closed heat and moisture regulated container (BlackBlock, BBKW, Lisbon, Portugal) according to Schmid et al., 2022. Ambient air was captured by 2 collectors and heated through solar irradiance. The heated air was then moved from the collectors into the chamber using in-line duct fans while air was circulated in the chamber using six fans. The drying process was controlled by a custom algorithm that ensured optimal drying parameters based on in- and outdoor temperature and humidity sensors. The chamber was equipped with a dehumidifier (TTK 350 S; 70 L/ 24 h, 1.3 kW, Trotec GmbH, Heinsberg, Germany) to regulate humidity and a fan heater (TDS 20; 3.3 kW, Trotec GmbH, Heinsberg, Germany) was present to ensure constant temperatures during night time. The dehumidifier was set to 25 % humidity (minimal operating value) and the maximum temperature was set to 40 °C (maximum operating value). The *C. vulgaris* paste was poured in 1 kg stainless steel trays (94 × 34 × 3.4 cm) covered with baking paper. The drying process continued for 21 h. Temperature and humidity sensors recorded a temperature and humidity oscillation between 25 and 35 °C and 20–30 % humidity, respectively, during most of the process.

2.3. Nutritional composition

The total protein content was measured by the Kjeldahl method using a Büchi Kjeldahl K-314 distillation unit (Büchi Labortechnik AG, Flawil, Switserland). Proteins are then calculated by multiplying the N content by a microalgae-specific conversion factor of 4.78 (Lourenço, Barbarino, Lavín, Lanfer Marquez, & Aidar, 2004). Lipid content was quantified using gas chromatography – flame ionization detection (GC-FID) analysis for total fatty acids quantification by chloroform/methanol extraction (2:1; v/v) (Clavijo Rivera et al., 2018). Total carbohydrates were quantified with the phenol–sulfuric acid method with a glucose calibration curve (Dubois, Gilles, Hamilton, Rebers, & Smith, 1956). Starch was enzymatically quantified with a Megazyme Total Starch Essay kit (Neogen Corporation, Lansing, MI, USA). Fiber content was measured using the Megazyme Total Dietary Fiber Assay kit (Neogen Corporation, Lansing, MI, USA). Ash content was determined by gravimetric method after incineration of the sample at 550 °C. The moisture content was measured gravimetrically, by drying at 70 °C under reduced pressure for 48 h.

2.4. Techno-functional properties

2.4.1. Protein and carbohydrate solubility

Samples were prepared as 2 % (w/v) in bidistilled water by magnetic stirring for 30 min. Then, the pH was adjusted to pH 7 with HCl (0.1 and 1 M) and NaOH (0.1 and 1 M) followed by 30 min of magnetic stirring. This was repeated 2 times to account for the buffering effect of the sample. Next, samples were centrifuged for 15 min at 10,000*g* (Sorvall™ LYNX 6000, Thermo Fisher Scientific, Waltham, MA, USA. Protein solubility was determined in triplicate with a bicinchoninic acid (BCA) protein assay kit (Merck Life Sciences, Darmstadt, Germany) using bovine serum albumin (BSA) as a calibration curve. Protein solubility was calculated as the ratio of BSA equivalents in the supernatant (10-

fold dilution) compared to the whole sample (same sample preparation up to the centrifugation step, 10-fold dilution). Carbohydrate solubility was determined in triplicate according the phenol–sulfuric acid method using glucose as a calibration curve (Dubois et al., 1956). Carbohydrate solubility was calculated as the ratio of glucose equivalents in the supernatant (50-fold dilution) to glucose equivalents in the whole biomass (same sample preparation up to the centrifugation step, 50-fold dilution).

2.4.2. Emulsifying capacity

Emulsifying capacity was determined in triplicate according to Benelhadj, Gharsallaoui, Degraeve, Attia, and Ghorbel (2016) and Schmid et al. (2022) with modifications. Suspensions containing 0.5 %, 1 %, and 2 % (w/v) microalgae in distilled water were magnetically stirred for 30 min and set to pH 7. For each concentration, 30 mL of sunflower oil (Boni, obtained from a local supermarket) was added to 30 mL of suspension and homogenized at 15,000 rpm with a rotor–stator disperser Ultra-Turrax T25 (Ika, Staufen, Germany) to form an oil-in-water emulsion. After homogenization, 10 mL of the emulsion was transferred into a 15 mL falcon tube and immediately centrifuged at 1500*g* for 5 min (Sorvall LYNX 6000, Thermo Fisher Scientific, Waltham, MA, USA). After centrifugation, the volume of emulsified fraction was recorded and EC was expressed as percentage of emulsified volume.

$$\textit{Emulsion capacity}\ [\%] = \frac{V_E}{V_T} \times 100$$

where V_E is volume of the emulsified fraction and V_T is the total volume (algal suspension + oil).

2.4.3. Foaming capacity and stability

Foaming properties were determined in triplicate according to Xiong, Xiong, Ge, Xia, Li, and Chen (2018) and Schmid et al. (2022) with modifications. Briefly, 0.15 g of microalgal powder was suspended in 15 mL of distilled water. Samples were stirred magnetically for 30 min and set to pH 7. Next, samples were whipped with a rotor–stator disperser Ultra-Turrax T25 (Ika, Staufen, Germany) at 8000 rpm for 1 min. Immediately after whipping, the foam was transferred to a 25 mL graduated cylinder. Foaming capacity was defined by the ratio of foam volume after 2 min and the initial sample volume. Foaming stability was determined by the ratio of the foam volume after 60 min and the initial foam volume.

$$\textit{Foaming capacity}\ [\%] = \frac{V_0}{15} \times 100$$

$$\textit{Foaming stability}\ [\%] = \frac{V_t}{V_0} \times 100$$

where V_0 is the foam volume after 2 min and V_t is the foam volume after 60 min.

2.4.4. Minimal gelling concentration

Minimum gelling concentration was determined in triplicate according to Sun and Arntfield (2010) with minor modifications. Microalgal suspensions were made at concentrations of 10–30 % (w/v) with 2 % increments and were set at pH 7. Suspensions were vortexed for at least 60 s (until all sample was dissolved). After homogenization, 5 mL of suspension was transferred to a sealed glass test tube and heated in a water bath (75 or 95 °C) for 10 min. Sample tubes were cooled at room temperature for 1 h and subsequently stored at 4 °C overnight. Next day, sample tubes were inverted and the sample with the lowest concentration that did not flow was regarded as the minimum gelling concentration.

2.4.5. Water and oil holding capacity

Water/oil holding capacity was determined in triplicate according to Stone, Karalash, Tyler, Warkentin, and Nickerson (2015) and Schmid et al. (2022). Briefly, 0.5 g of microalgal powder was suspended in 10 mL of distilled water (and set to pH 7) or sunflower oil in a 50 mL falcon tube. During a 30 min period, samples were vortexed for 10 s every 5 min, followed by centrifugation at 1000*g* for 15 min at room temperature (Sorvall LYNX 6000, Thermo Fisher Scientific, Waltham, MA, USA). After centrifugation, the supernatant was carefully decanted to remove any unbound water or oil and the remaining pellet was weighed. Results were expressed as g water/g DW or g oil/g DW.

$$\textit{Water or Oil holding capacity} = \frac{w - w_0}{w_0}$$

where w is the weight of the pellet after centrifugation and suspension in water or oil. w_0 is the initial weight of microalgal powder.

2.4.6. Water solubility index

Water solubility index was determined in triplicate according to Calderón-Castro et al. (2019) and Schmid et al. (2022). Briefly, 0.5 g of dried microalgal powder was suspended in 10 mL of distilled water in a 50 mL falcon tube. Samples were magnetically stirred for 30 min and set to pH 7, followed by centrifugation at 1800*g* for 15 min at room temperature (Sorvall LYNX 6000, Thermo Fisher Scientific, Waltham, MA, USA). After centrifugation, the supernatant was decanted in a metal dish and the residue was weighed after drying for 12 h at 105 °C.

$$\textit{Water solubility index}\ [\%] = \frac{w_S}{w_0} \times 100$$

where w_S is the weight of the dried supernatant and w_0 is the initial weight of the microalgae powder.

2.5. Protein denaturation

To evaluate protein denaturation, differential scanning calorimetry (DSC) was used to analyze samples in triplicate according to Verfaillie, Janssen, Van Royen, and Wouters (2023) with modifications. Approximately 10 mg of a 30 % w/w solution of microalgae in distilled water was loaded in to aluminum Tzero hermetic pans (TA Instruments, Waltham, MA, USA). An empty reference pan was measured in every run. The degree of protein denaturation was determined by heating from 20 °C to 120 °C at a rate of 5 °C/min using a DSC Q2000 system (TA Instruments, Waltham, MA, USA). The energy flow was plotted in function of temperature using Universal Analysis 2000 software (TA Instruments, Waltham, MA, USA). Using the same software, denaturation peaks were manually integrated and converted to a denaturation enthalpy/ g DW as well as a denaturation temperature.

2.6. Particle size distribution analysis

The particle size distribution analysis was performed in 5-fold by laser diffraction spectrometer Mastersizer 3000 (Malvern Panalytical, Worcestershire, UK) based on the method of Carullo et al., 2018. The powder samples were solubilized in bidistilled water (2 % w/v) and stirred magnetically for 30 min before dispersion in the aqueous dispersion unit (Hydro MV, Malvern Panalytical) filled with distilled water. Sample was added until an obscuration of 9 % was reached 9 % ± 3 % and the particle size distribution was determined using the Fraunhofer approximation with water as a dispersant medium (refraction index = 1.33). Mean particle size was expressed as volume mean diameter ($D_{4,3}$) that was automatically calculated by the Mastersizer 3000 software.

2.7. Color determination (L*-,a*-,b*- values)

Color determination of the powders (L*a*b* values; n = 15) was done using a CM-600d colorimeter (Konica Minolta, Tokyo, Japan)

under standardized light D65 in a glass cuvette (CR-A504, Ø 34 mm, Konica Minolta, Tokyo, Japan). The cuvette was covered with the white calibration plate to prevent the measurement from being disturbed by reflecting light. The Euclidean color distance ΔE was calculated according to the following equation.

$$\Delta E = \sqrt{(L_C^* - L_S^*)^2 + (a_C^* - a_S^*)^2 + (b_C^* - b_S^*)^2}$$

where L_C^*, a_C^*, b_C^* and L_S^*, a_S^*, b_S^* are the L*a*b*-values of the control and the sample to compare respectively.

2.8. Microscopic imaging

Microalgal cell structure was visualized by phase-contrast light microscopy using an optical microscope (Leica Diaplan, Wetzlar, Germany). Sample powders were solubilized in bistilled water (0.05 % w/v) and stirred for 30 min. Images were taken at a magnification of 800 × (8 × eyepiece, 100 × objective) using immersion oil.

2.9. In vitro protein digestibility

Protein digestibility was evaluated with the harmonized and revised *in vitro* digestion protocol INFOGEST 2.0 (Brodkorb et al., 2019; Minekus et al., 2014). All enzymes and reagents used in this protocol were obtained from Merck Life Science (Darmstadt, Germany). Each experiment included blank controls containing digestive fluids, enzymes and bile to correct for nutrients not originating from the sample. Distilled water was added to the dried powder in a 3:2 ratio to obtain a final weight of 2.5 g of starting material resulting in a final 20 mL of intestinal phase. During the oral phase, simulated salivary fluid was added but no salivary amylase (optional). In the gastric phase, porcine pepsin (2000 U/mL) and gastric simulated fluid were added but no gastric lipase (optional step). In the intestinal phase, porcine pancreatin (100 U/mL) was added as well as bovine bile (10 mM). Finally, a protease inhibitor (Bowman-Birk Inhibitor, 0.05 g/l, 100 μL per ml digest) was added at the end of the protocol to irreversibly inhibit trypsin activity. The final volume of the digest amounted to 22 mL. After halting protein proteolysis, samples were centrifuged for 15 min at 10,000*g* (Sorvall LYNX 6000, Thermo Fisher Scientific, Waltham, MA, USA) to separate indigestible protein (non-soluble) from digested protein and the supernatant was stored at −80 °C until further analysis. Digestion was performed in triplicate for each sample.

2.9.1. Degree of hydrolysis

The degree of protein hydrolysis (DH) was estimated by measuring the free amino groups in the digest supernatant. Therefore, the 2,4,6-trinitrobenzenesulfonic acid (TNBS) method was used based on the method of Adler-Nissen, 1979. Samples were diluted 100-fold in 1 % sodium dodecyl sulfate solution and subsequently suspended in a mixture of 0.2125 M pH 8.2 phosphate buffer and 0.1 % (w/v) TNBS solution. Next, samples were incubated in the dark at 50 °C for 60 min and the reaction was stopped with 0.1 M HCl. Absorbance was measured at 340 nm (Jasco V-760, JASCO Applied Sciences, Halifax, Canada) and the primary amino group concentration was calculated based on a glycine calibration series, with correction based on the blanks. The DH could then be estimated by dividing the number of hydrolyzed peptide bonds (h) by the initial amount of peptide bonds present in the sample (h_{tot}). The estimation of h_{tot} was taken from literature as the approximate value of 8.2 mmol/$g_{protein}$ (Adler-Nissen, 1979; Rieder et al., 2021). Each digest was analyzed in triplicate (3 digestions per sample).

2.9.2. Nitrogen solubility

The amount of solubilized nitrogen (N-solubility) in the digest supernatant was determined through the Kjeldahl method based on the protocol of Broucke et al., 2022 with modifications. Briefly, 2.5 g of supernatant was hydrolyzed by sulfuric acid and heating up to 300 °C for 20 min and 420 °C for 1 h and 50 min. The residue was analyzed for nitrogen in an automated Kjeltec 8400 device (FOSS, Hillerød, Denmark). The obtained nitrogen value was divided by the sample's original nitrogen content (see 2.3) to obtain the N-solubility value. Each digest was analyzed in singular (3 digestions per drying method).

2.10. Sensory evaluation

To evaluate of the effect of the drying method on the sensory properties of *C. vulgaris*, a trained expert panel and taste lab were used as described in Coleman et al., 2022. Seven trained assessors participated in the sensory evaluation. Prior to the sensory assessment, an exploratory session was organized to identify sensory attributes of the different *C. vulgaris* powders. Several attributes including taste and odor were selected based on the panel discussion (Table 1). A concentration of 10 g/L DW and 50 g/L DW were deemed satisfactory for evaluation of taste and smell attributes respectively. Solutions were prepared in advance of the sensory assessment using mineral water (Cristaline, Sources-Alma, France) and small volumes (20 mL) of sample solutions were presented in randomly coded and closed 30 mL screw-capped amber colored glass vials. Separate sessions were held for taste and smell attributes to prevent saturation of the senses.

Ethical statement

All sensory research performed in this study was in accordance with Ethical Standards of the Commission of Flavor and Odor of ILVO (ECSG-ILVO) according to Coleman et al., 2022. Samples were tested on microbial safety (yeast and molds enumerations, coagulase positive *S. aureus* enumerations, *E. coli* enumerations, *Salmonella* spp. detection, *Listeria* spp. and *L. monocytogenes*. detection), heavy metals analysis (Cd, Pb, Hg, total As, inorganic As and I). A food grade production statement of *C. vulgaris* biomass was provided by Allmicroalgae S.A. A risk evaluation based on these data was made and was evaluated by the ECGS-ILVO. Participants gave their informed consent and were able to withdraw from the study at any time. Results were handled confidentially.

2.11. VOC analysis

To determine the effect of the different drying methods on the chemical aroma profile, volatile organic compounds (VOCs) were determined using automated headspace solid-phase microextraction (HS-SPME) – gas chromatography-mass spectrometry (GC–MS) according to Coleman et al., 2022. Three replicate analyses were performed on each sample on different days. The concentration of each VOC was semi-quantitatively calculated by multiplying the obtained responses with the concentration of internal standard in the samples (6.8 μg/L 2-methyl-3-heptanone and 72.9 μg/L methyl nonanoate). These concentrations were divided by their individual odor threshold value (OTV) to calculate the odor activity values (OAVs) of each volatile according to Coleman et al., 2022. OTVs were sourced from literature (Suppl. Data, Table 1).

2.12. Statistical analysis

Significant differences (except for sensorial and VOC data) were

Table 1
Sensory attributes associated with the *C. vulgaris* samples together with their odor/taste description.

Sensory attributes	Description
Umami taste	The taste associated with monosodium glutamate
Sour taste	The taste associated with citric acid
Bitter taste	The taste associated with caffeine
Yeast odor	The odor associated with nutritional yeast
Cacao odor/taste	The odor/taste associated with cacao powder
Earthy odor/taste	The odor/taste associated with beetroot

determined by performing a one-way ANOVA followed by a Tukey post-hoc multiple comparison at the $\alpha = 0.05$ significance level using the statistical software R (version 4.0.3) (R Core Team. (2020), 2020). Statistical analyses on the sensorial and VOC data were performed according to Coleman et al., 2023. For sensorial analyses, significant differences for each attribute between different drying methods were determined with a linear mixed-effect model (lmer function, "lsmeans" package) (Lenth, 2016). The effect of the panelists was considered random. A type-III ANOVA with $\alpha = 0.05$ was performed subsequently. Principal component analysis (PCA) was performed using MetaboAnalyst (version 5.0) to reduce dimensionality and visualize differences in the sensorial data (mean-centered) and in the VOC data (mean-centered and log-transformed). Correlations between odor attribute scores of the sensorial evaluation and individual VOCs were assessed using partial least-squares regression (PLSR) (plsr function, "pls" package) (Liland, Mevik, & Wehrens, 2022). The PLSR was applied on the mean odor attribute scores and the mean-centered, log-transformed OAVs of the VOCs with leave-one-out cross-validation. The correlation coefficients obtained from the PLSR analysis were visualized in a heatmap using MetaboAnalyst (version 5.0).

3. Results & discussion

3.1. Nutritional composition

The proximate composition of powders is listed in Table 2. All drying methods resulted in powders with acceptable moisture contents of <10 % and a_w <0.6 to avoid microbial growth (Vera Zambrano et al., 2019). Differences between differently dried samples were limited although in some cases significant ($p < 0.05$). The protein content of the samples ranged between 18.2 and 19.7 %. The biomass additionally consisted of approximately 50–54 % carbohydrates, with 20–25 % of this content attributed to dietary fiber. These findings are in line with other studies on heterotrophic *C. vulgaris* species with protein content typically on the lower side (<20 %), whilst the biomass was predominantly comprised of carbohydrates (Canelli et al., 2021; Rattanapoltee & Kaewkannetra, 2014). Further, low quantities of both lipids (<8 %) and ash (<5 %) were found. However, ATFD resulted in significantly ($p < 0.05$) lower dietary fiber content (5.7 %) compared to other samples (19.2–25.5 %). We hypothesized that this could be caused by losses during drying, because lumps of aggregated material were found during drying that were removed by sieving to obtain a homogenous powder. Moreover, a reduction in lipid content was also observed after ATFD. Besides protein content, essential amino acid content (EAA) is an important measure of nutritional quality. Heterotrophic *C. vulgaris* was characterized by high EAA content (35.7 g/ 100 g protein) (Suppl. data, Table 1). Based on the latest WHO/FAO guidelines for amino acid requirements in human adults, heterotrophic *C. vulgaris* protein was only deficient in 1 of the 9 given EAAs (isoleucine).

3.2. Techno-functional properties

The dried *C. vulgaris* powders and their color difference are shown in Fig. 1**a**. The dried material showed visual differences such as a lighter color for ATFD, a greener color after FD and darker color after SolD, PCD and SprD. The L*-,a*-,b*-values as well as ΔE are shown in Fig. 1**b**. The samples are arranged in order of rising ΔE (SprD < PCD < ATFD < SolD) in comparison to the mildest drying treatment FD. Here, a higher value of ΔE represents a larger color difference compared to FD, which indicated a higher impact on color after SolD and ATFD. The visual lighter color after ATFD was confirmed by a significantly higher L*-value. Furthermore, a higher a*-value indicated a reduction in green color for all samples compared to FD, which implied higher chlorophyll preservation in the FD sample.

The impact of drying on the different functional properties of *C. vulgaris* was determined and compared with traditional protein sources including a commercial soy isolate (SI) and egg white isolate (EWI) (Table 3**)**. ATFD led to an improvement of several water-related techno-functional properties including gelling properties, water holding properties and solubility. Minimal gelling concentration was lowest after ATFD with 20 % (w/v) and 15 % (w/v), at 75 °C and 95 °C respectively (Table 3). The improved gelling properties after ATFD compared to other drying methods could be related to a significant increase ($p < 0.05$) of the free carbohydrates (Fig. 2), as long chain carbohydrates have the ability to molecularly interact to form a three-dimensional network (Saha & Bhattacharya, 2010). In addition, microscopic images revealed a loss of cell structure in most *C. vulgaris* cells after ATFD, whereas cells remained mostly intact after the other drying methods (Fig. 1**c**). Loss of cell structure could lead to the release of free carbohydrates and proteins from the cytoplasm and the cell wall as well as other cell constituents, which might have improved gelling capability (Azmi, 2020). Additionally, DSC analysis showed significantly decreased denaturation enthalpy ($p < 0.05$) after ATFD, which indicates partial denaturation of proteins (Table 4). Protein denaturation increases exposure of hydrophobic regions which are mostly at the core of the protein in native state, which in turn promotes network formation by interactions with other molecules (Brodkorb et al., 2016). Shkolnikov Lozober, Okun, & Shpigelman, 2021 reported an increase in gelling capabilities of the cyanobacterium *Arthrospira platensis* after high pressure homogenization to disrupt the cells. However, the increased gelling capability was attributed to an increase in protein solubility which was not observed here (Fig. 2). *C. vulgaris* generally showed inferior gelling properties compared to the traditional protein isolates with a minimal gelling concentration (95 °C) of 10 % and 6 % for the commercial SI and EWI, respectively. This shows that treatments (such as ATFD) to improve the gelling properties might be desirable to increase competitiveness of microalgae as functional ingredients.

Besides gelling abilities, also a higher water binding and water solubility properties were observed after AFTD compared to other drying methods (Table 3). Water holding capacity was significantly increased ($p < 0.05$) after AFTD compared to the other drying methods. Water binding properties are primarily related polar hydrophilic groups that allow hydrogen bonding with water molecules, which is dependent on amino acid composition and protein conformation (Zayas, 1997). Thermal protein denaturation of soy protein was found to increase the water holding capacity, which likely explains the increased water holding capacity after ATFD given the significant protein denaturation (Table 4) (Zheng et al., 2019). Water holding capacity of *C. vulgaris* is

Table 2
Proximate composition of dried *C. vulgaris* powders (replicates n = 3).

g/100 g	FD	SprD	ATFD	PCD	SolD
Protein (N x 4.78)	19.7 ± 0.6^{a}	18.4 ± 0.5^{ab}	19.1 ± 0.5^{ab}	19.2 ± 0.5^{ab}	18.2 ± 0.5^{b}
Carbohydrates	51.3 ± 0.4^{b}	51.6 ± 0.3^{b}	49.9 ± 0.4^{c}	53.8 ± 0.4^{a}	51.7 ± 0.2^{b}
Of which starch	27.5 ± 1.1^{ab}	29.6 ± 3.3^{a}	21.6 ± 1.5^{b}	27.3 ± 3.1^{ab}	34.5 ± 3.8^{a}
Of which fiber	19.2 ± 2.8^{a}	24.8 ± 3.1^{a}	5.7 ± 1.6^{b}	25.5 ± 3.2^{a}	19.6 ± 2.8^{a}
Lipids	6.1 ± 0.4^{a}	7.2 ± 0.8^{a}	3.1 ± 0.3^{b}	7.1 ± 0.5^{a}	5.5 ± 0.3^{a}
Ash	3.4 ± 0.2^{b}	3.6 ± 0.3^{ab}	4.1 ± 0.3^{ab}	4.4 ± 0.3^{a}	3.5 ± 0.2^{b}
Moisture	3.7 ± 0.5^{c}	3.0 ± 0.5^{c}	5.3 ± 0.5^{b}	2.7 ± 0.5^{c}	7.2 ± 0.5^{a}
a_w	0.12	0.09	0.26	0.07	0.49

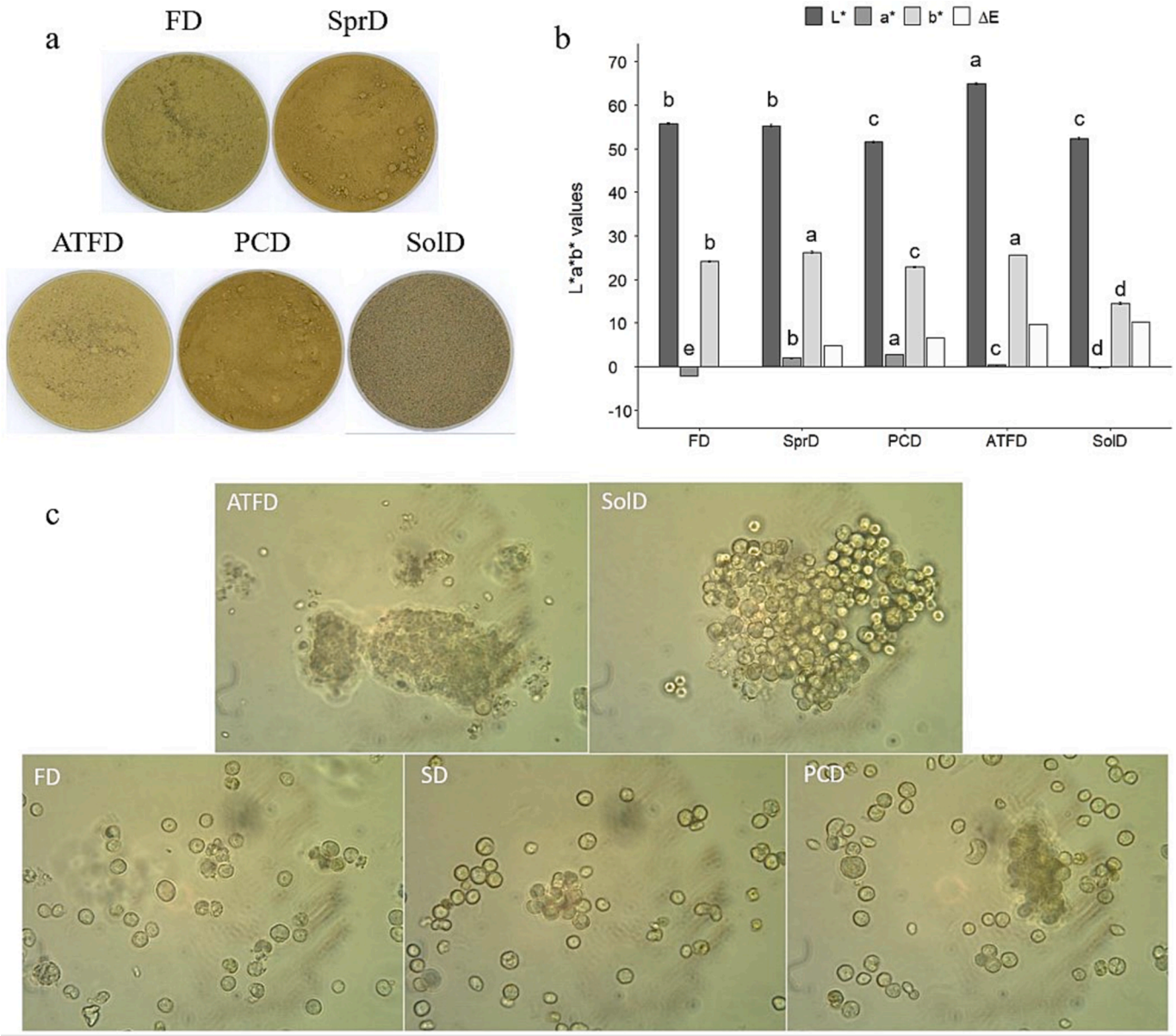

Fig. 1. Powders of dried *C. vulgaris* after agitated thin film drying (ATFD), solar drying (SolD), freeze drying (FD), spray drying (SprD) and pulse combustion drying (PCD) (a), L*a*b* color determination of dried powders (n = 15) (b), Phase-contrast microscopic images (800 × magnification) of *C. vulgaris* of dried powders in suspension (0.05 % w/v) (c). Significant differences in L*a*b*-values are indicated with different lowercase letters.

low compared to the commercial SI, but considerably higher than the EWI. The study of Guil-Guerrero et al. (2004) considered the water holding capacity of several freeze-dried microalgae (*Porphyridium cruentum*, *Nannochloropsis* spp. and *Phaeodactylum tricornutum*) powders which also exhibited increased water holding capacity (4.0–8.1 g/g) compared to the biomass in this study. The water solubility index, which represents the proportion of all soluble components in the sample, was significantly increased ($p < 0.05$) after ATFD. SolD resulted in a powder with the lowest water solubility index, which coincides with the significantly lower protein and carbohydrate solubility (Fig. 2). The increase in total solubility after ATFD was likely related to the increase in soluble carbohydrates, although other cell constituents might also have been solubilized. Solubilized proteins are also able to interact with water and air to form and stabilize foams at the air–water interface (Zayas, 1997). The foaming capacity of heterotrophic *C. vulgaris* powders ranged from 13 to 33 %. This demonstrates the relatively limited foaming abilities of this microalgae in comparison to the SI and EWI (89–102 %). Higher foaming capacity for other microalgal species such as *A. platensis* (101–246 %) were reported (Lupatini Menegotto et al., 2019). Nevertheless, protein sources with reduced foaming properties might be beneficial for some applications where strong foaming is undesirable, e.g. in meat alternatives where a dense and firm structure is often preferred.

Protein solubility was not increased after ATFD (Fig. 2), despite indications of cell disruption (Fig. 1**c**). Microalgal protein solubility typically increases following cell disruption treatment by releasing proteins from the cytosol (Soto-Sierra, Stoykova, & Nikolov, 2018). Besides decreased denaturation enthalpy after ATFD, denaturation temperature also decreased significantly ($p < 0.05$), indicating reduced thermal protein stability. Decreased denaturation enthalpy, corresponding to protein unfolding, can decrease protein solubility. This is mediated by aggregation, as hydrophobic groups and sulfhydryl groups become available for non-covalent and covalent intermolecular interactions, respectively (Wijayanti, Brodkorb, Hogan, & Murphy, 2019). As such, the expected increase in protein solubility due to cell rupture is likely offset by aggregation. Cell debris aggregation after ATFD was observed

Table 3
Techno-functional properties of dried *C.* vulgaris powders, recalculated for dry weight. Commercial soy isolate (SI) and egg white protein isolate (EWI) results are included as a reference. The functional properties values represent the average of 3 measurements for each drying treatment. Significant differences between drying treatment for each functional property are represented by different lowercase letters. SI an EWI are not included in statistical comparisons.

Drying treatment	Emulsion capacity (%)			Foaming capacity (%)	Foaming stability (%)	Minimal gelling concentration (%)		Water holding cap. (g/g)	Oil holding cap. (g/g)	Water solubility index (%)
g/ 100 mL	**0.5**	**1**	**2**							
Temperature						**75 °C**	**95 °C**			
FD	51.3 ± 1.5^{a}	51.4 ± 1.5^{ab}	54.3 ± 1.3^{a}	16.5 ± 2.0^{bc}	71. ± 10.4	> 30	22	1.0 ± 0.1^{c}	0.8 ± 0.1^{a}	27.6 ± 0.2^{b}
SprD	0	31.1 ± 0.9^{d}	48.5 ± 1.5^{b}	23.4 ± 4.1^{b}	69.4 ± 4.4	> 30	> 30	1.0 ± 0.1^{bc}	0.3 ± 0.1^{d}	25.8 ± 0.1^{c}
ATFD	0	47.8 ± 1.5^{b}	52.1 ± 1.5^{ab}	13.2 ± 2.1^{c}	100.0 ± 0.0	20	15	1.5 ± 0.1^{a}	0.6 ± 0.1^{b}	32.2 ± 0.5^{a}
PCD	0	39.0 ± 1.9^{c}	44.1 ± 1.7^{c}	32.7 ± 2.0^{a}	74.8 ± 7.1	> 30	> 30	1.0 ± 0.1^{bc}	0.9 ± 0.1^{a}	27.7 ± 0.1^{b}
SolD	9.0 ± 3.0^{b}	53.0 ± 1.5^{a}	55.7 ± 1.6^{a}	15.8 ± 2.1^{c}	70.0 ± 8.7	> 30	26	1.1 ± 0.1^{b}	0.5 ± 0.1^{c}	22.2 ± 0.9^{d}
SI	55.0 ± 2.2	57.3 ± 2.1	60.8 ± 2.0	88.9 ± 3.9	93.8 ± 2.1	12	10	8.7 ± 0.1	1.0 ± 0.1	21.8 ± 0.4
EWI	54.5 ± 1.4	54.2 ± 0.7	53.8 ± 1.2	102.2 ± 3.9	85.8 ± 2.2	8	6	0.1 ± 0.1	0.9 ± 0.1	90.0 ± 1.2

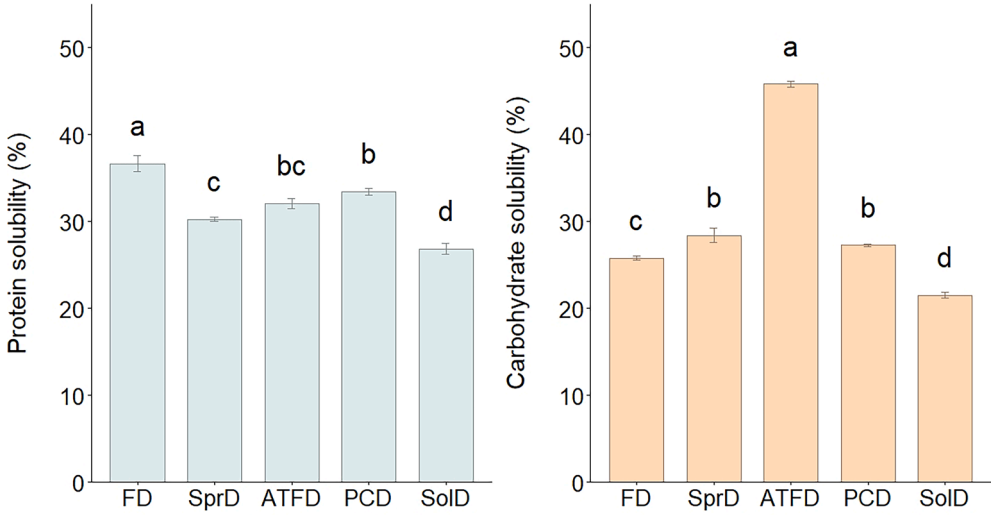

Fig. 2. Protein and carbohydrate solubility (n = 3) at pH 7 after centrifugation at 10,000*g* for 2 % (w/v) solutions of dried *C. vulgaris* powders. Significant differences in protein solubility and carbohydrate solubility of the samples are indicated with different lowercase letters.

Table 4
Thermal properties of *C. vulgaris* dried powders derived from differential scanning calorimetry thermograms. Denaturation enthalpy (ΔH) and denaturation temperature (T_d) values represent the average of 3 measurements. The value of ΔH is expressed as J per gram of dry biomass. Significant differences are indicated with different lowercase letters.

	Denaturation enthalpy ΔH (J/g DW)	Denaturation temperature T_d (°C)
FD	5.01 ± 0.16^{a}	80.17 ± 0.13^{b}
SprD	4.96 ± 0.17^{a}	81.12 ± 0.16^{a}
ATFD	2.74 ± 0.13^{b}	75.60 ± 0.04^{d}
PCD	4.95 ± 0.14^{a}	81.29 ± 0.02^{a}
SolD	5.07 ± 0.11^{a}	79.86 ± 0.02^{c}

in the microscopic images (Fig. 1), as well as a significant increase ($p < 0.05$) in average particle size compared to the other drying methods (Fig. 3). The average particle size of the ATFD sample (22.7 μm) was well above the cell size of a *C. vulgaris* cell (2–10 μm), whereas the particle size for the other drying methods approximated the *C. vulgaris* cell size (4.7–9.0 μm). These data suggest aggregation of cellular

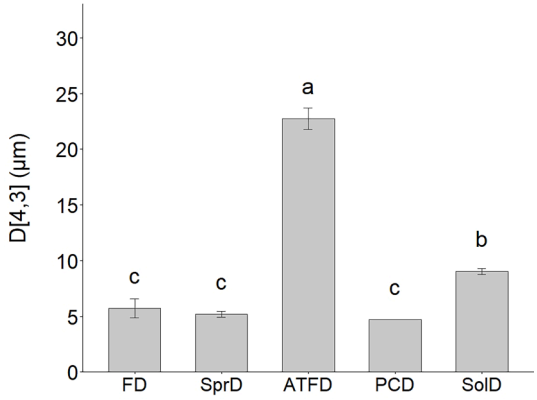

Fig. 3. Average particle size (d_{43}) (n = 5) at pH 7 of 2 % (w/v) solutions of dried *C. vulgaris* powders. Significant differences in average particle size are indicated with different lowercase letters.

material during ATFD, which likely contributes to the sequestering of free protein.

The emulsion capacity was significantly higher ($p < 0.05$) after FD at the lowest powder concentration (0.5 % w/v) compared to the other drying methods, indicating increased emulsifying abilities (Table 3). Emulsion capacity increased after ATFD and SolD to similar levels as FD at the 1 and 2 % (w/v) concentration. Compared to the commercial EWI and SI, the emulsion capacity after FD is similar at 0.5 % (w/v) concentration. This coincided with a significantly higher protein solubility ($p < 0.05$) associated with the FD treatment (Fig. 2). Protein solubility in the aqueous phase is positively correlated to the protein diffusion rate to the oil–water interphase. This enhances interfacial protein film formation and likely explains the improved emulsion capacity after FD (Lam & Nickerson, 2013).

The oil holding capacity was highest ($p < 0.05$) after FD and PCD (0.8 g/g), similar to the oil holding capacity of SI and EWI (Table 3). This shows that using FD and PCD to dry heterotrophic *C. vulgaris* results in competitive fat-binding properties compared to these conventional protein sources. Differences in oil holding capacity after drying could originate from exposure of non-polar amino acid sidechains that leads to differences in protein surface hydrophobicity (Acquah et al., 2021). Differences in powder particle structure could also influence physical entrapment of oil in the microstructure (Zayas, 1997).

In conclusion, these data show improved gelling and water binding capabilities after ATFD. In contrast, the functional properties were generally limited after SolD, SprD and PCD. FD resulted in increased lipid-related properties such as emulsifying and fat binding abilities compared to the other drying methods. Dried heterotrophic *C. vulgaris* powders exhibited similar emulsion capacity and oil holding capacity compared to traditional high-protein sources such as SI and EWI. These favorable lipid-related properties make it an interesting functional ingredient for emulsified meat analogues or oil-in-water emulsions such as sauces or dressings. Nonetheless, for other functional properties such as water holding, foaming and gelling properties, this novel source of single-cell protein is less competitive compared to the commercial soy and egg white isolate included in this study. However, there is potential for techno-functional properties to be further improved upon disrupting the microalgal cell wall, a likely limiting factor, through various cell disruption techniques as well as further protein purification (Acquah et al., 2021).

3.3. *In vitro protein digestibility*

The N-solubility and degree of protein hydrolysis(DH) are represented in Fig. 4. The N-solubility is a measure for solubilized protein, oligo-, tri- and dipeptides as well as single amino acids. The result of this method is often referred to as the *in vitro* protein digestibility (IVPD) and is commonly used to describe microalgae digestibility (Van De Walle et al., 2023). N-solubility was significantly ($p < 0.05$) higher after ATFD (80.3 %) compared to the other drying methods (64.7 – 69.8 %) (Fig. 4b). Yet, N solubility of the *C. vulgaris* powders remained low compared to SI (94 %) and EWI (97 %). The increased N-solubility after ATFD was likely attributable to loss of the cell structure (Fig. 1**c**), which enhances the bioavailability of proteins for digestive enzymes, consequently leading to an improvement in protein digestibility (Teuling et al., 2017; Van De Walle et al., 2023). Protein denaturation of the ATFD *C. vulgaris* sample (Table 4) could also increase digestive enzyme accessibility through a mechanism of protein unfolding while protein aggregation caused by denaturation would reduce this effect (Yin, Tang, Wen, Yang, & Li, 2008). These data suggest improved protein digestibility after ATFD, in respect to the other drying techniques. Yet, a translation to *in vivo* digestibility and bioavailability of small peptides and amino acids in the intestine is challenging and requires further investigation.

The DH is a measure for the proportion of peptide bonds that are hydrolyzed upon digestion of the protein, resulting in free amino groups (in the form of oligo-, tri-, or dipeptides as well as free amino acids). The heterotrophic *C. vulgaris* degree of protein hydrolysis ranged from 39.5 to 44.9 % with no significant differences (Fig. 4a). This is comparable to the DH of casein (48 %) obtained with the same digestion and quantification method in the study of Rieder et al., 2021, with casein being regarded as a protein that is completely digestible. Digestion of the commercial SI and EWI resulted in a degree of protein hydrolysis of 38 % and 44 %, respectively, indicating relatively good *in vitro* digestion of *C. vulgaris*. It must be noted that the DH is typically lower than other measures of protein digestibility (such as N-solubility) because intestinal digestive enzymes activity mainly leads to oligopeptides of 2–6 amino acids long (Freeman, Kim, & Sleisenger, 1979). Complete digestion requires the activity of brush border peptidases, originating from the small intestine brush border membrane, which are not included in the INFOGEST 2.0 method (Rieder et al., 2021). Nonetheless, this quantification can be used to compare the protein digestibility after different treatments. Although no differences were found in the DH, the N-solubility data suggests improved bioavailability of protein after ATFD and *in vitro* digestion.

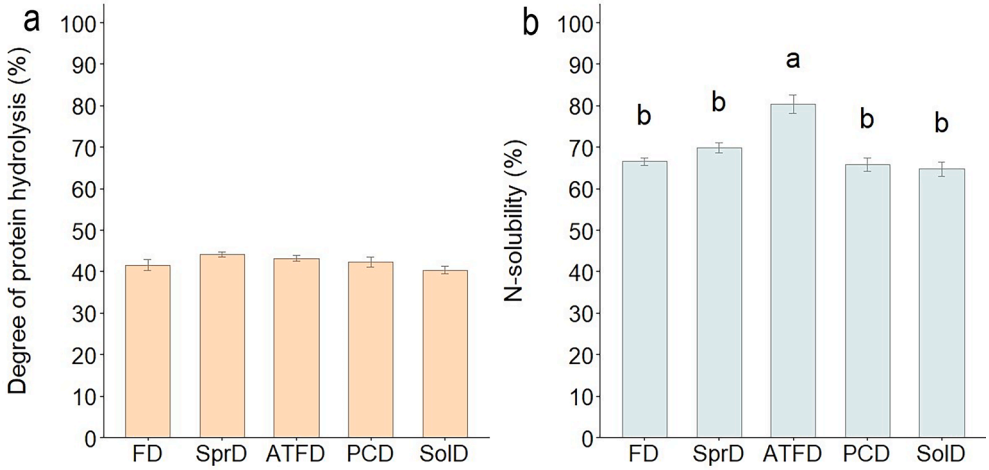

Fig. 4. Estimation of *C. vulgaris* protein digestibility after *in vitro* digestion using the INFOGEST 2.0 protocol, expressed as degree of protein hydrolysis (DH) (a) and expressed as N-solubility (b). Significant differences in N-solubility are indicated with different lowercase letters. The DH and N-solubility values represent the mean of triplicate measurements for 3 digestions (n = 9).

3.4. Sensory profiling

Differences in drying method lead to variations in the flavor profiles of microalgae *Nannochloropsis* sp. (Coleman et al., 2023). To evaluate the effect of the five different drying techniques used in this study on the sensory properties of heterotrophic *C. vulgaris*, a sensory evaluation using a trained taste panel was performed. The sensory evaluation indicated that ATFD significantly ($p < 0.05$) increased the earthy taste compared to SprD (Fig. 5a). PCD resulted in a significantly ($p < 0.05$) increased cacao odor compared to FD. These differences are also observable in the principal component analysis (PCA) plot (Fig. 5b). The sensory profiling indicated limited differences between PCD and SolD for most of the attributes, which is also visible in the PCA plot as a close clustering of the two drying techniques. No other significant differences were found between the sensory attributes of the different heterotrophic *C. vulgaris*. FD generally resulted in the lowest scores for all attributes, suggesting that this mild drying treatment led to a less intense flavor profile compared to the other treatments where heat was involved. A recent study by Grossmann, Wörner, Hinrichs, and Weiss (2020) did not remark any specific flavors in a lyophilized heterotrophic *Chlorella protothecoides* protein extract besides the basic tastes features (sweet, bitter, sour, salt, umami). Another study by Coleman et al. (2022) described the flavor profile of lyophilized autotrophic *C. vulgaris* as mostly earthy and grassy in nature.

VOC analysis resulted in identification of a total of 44 compounds in the 5 dried samples (Suppl. data, Table 2). The sulfur-containing compounds (methanethiol, dimethyl sulfide, dimethyl disulfide), alkyl aldehydes (2-methyl propanal, 3-methyl butanal, 2-methyl butanal), aldehydes (pentanal, hexanal) and 2,3-butanedione showed the OAVs, indicating that these compounds most likely contribute considerably to the odor profile of dried heterotrophic *C. vulgaris*. The strong presence of 2,3-butanedione, which is associated with a buttery smell, is a typical volatile compound normally associated with fermentation (Birch, Petersen, Arneborg, & Hansen, 2013).

The differences in VOC profile between different drying treatments are presented in Fig. 6. In general, FD exhibited the lowest OAVs for most of the VOCs, which correlates with the lower flavor and odor intensities perceived during the sensory evaluation (Fig. 5a). ATFD resulted in an increase of alcohols (1-octen-3-ol, 3-methyl-1-butanol), hexanal, 2-heptanone and safranal. The substantial increase in 1-octen-3-ol indicated lipid oxidation during ATFD, taking into consideration that drying was performed at 98 °C (for 10 min). There was also indication of cell disruption after ATFD (Figs. 1 and 2), which has been linked to increased lipid oxidation in *Nannochloropsis* sp. (Coleman et al., 2023). More so, 1-octen-3-ol is linked to earthy/mushroom smell, an aroma that was found to be enhanced in the sensory analysis after ATFD. PCD and, to a lesser degree, SprD displayed increased levels of alkyl aldehydes (2-methyl propanal, 2- and 3-methylbutanal) and furans (2- and 3-methylfuran, 2-ethylfuran, 2,5-dimethylfuran). Alkyl aldehydes (or Strecker aldehydes) and furans are formed during Maillard reactions at high temperatures that mainly originate from amino acids (protein), carbohydrates and fatty acids (Crews & Castle, 2007; Mottram, 2007). PCD and SprD likely promoted Maillard reactions with air temperatures reaching 600–800 °C and 200 °C, respectively, which could lead to momentary elevations in product temperature. The product temperature was likely not in the same range as the air temperature due to evaporation subtracting heat from the product and due to the absence of a burnt smell in the samples. The Strecker aldehydes and furans were generally associated with cocoa-like odors, but are also commonly linked to yeast aroma (Coleman, 2023). This suggested that the higher perceived cacao smell during sensory profiling for PCD was likely elicited by these VOCs. Solar drying resulted in an observable increase in dimethyl disulfide and isoamyl acetate. The former being associated with a garlic, onion-like odor while the latter is an ester that provides a

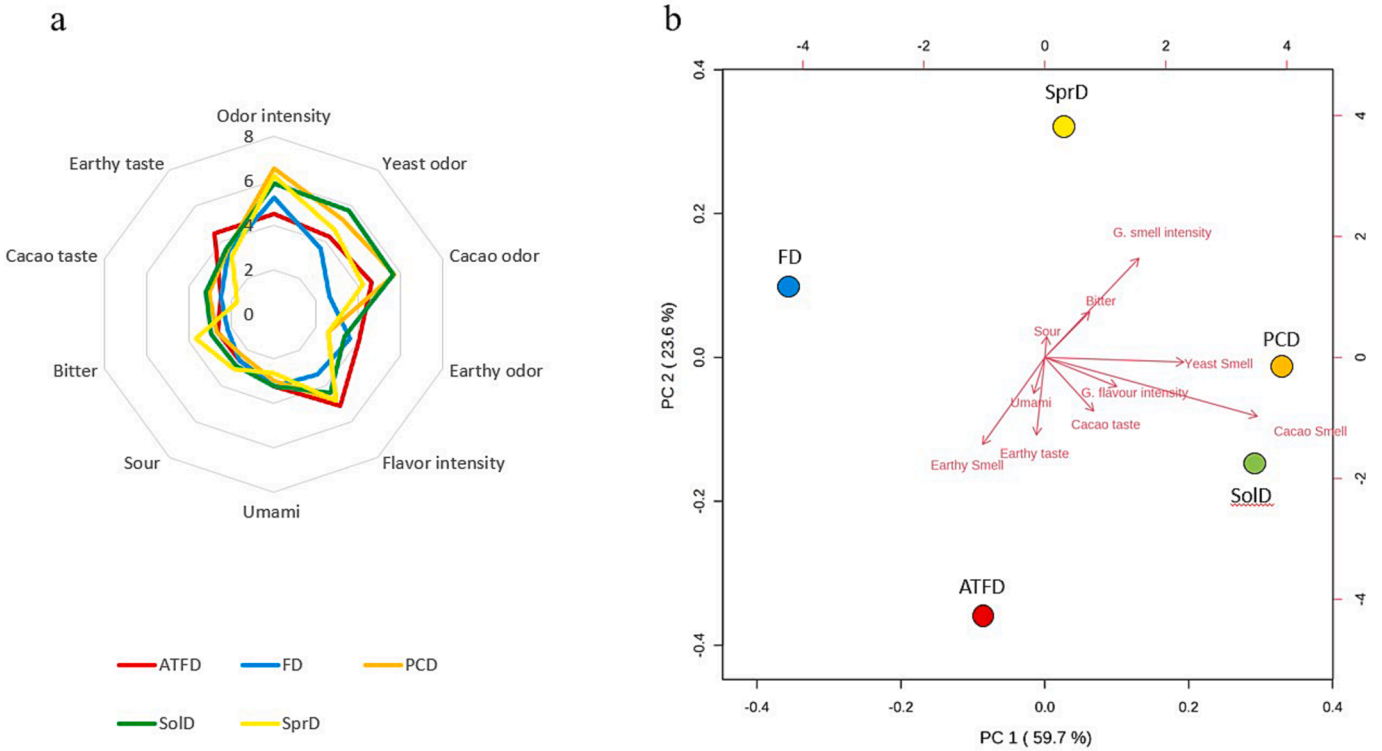

Fig. 5. Sensory evaluation of dried heterotrophic *C. vulgaris* biomasses visualized on a radar chart (a) and visualized on a PCA scores plot (b). The first 2 principal components of the PCA plot explain 83.3 % of the variance. Average scores of panelists (n = 7) were used and displayed. The sensory attributes are represented by red arrows. The evaluation criteria for the sensory attributes are presented in Table 1, which the judges were familiarized with. Scoring was performed relative between the samples, not in comparison to standards. (For interpretation of the references to color in this figure legend, the reader is referred to the web version of this article.)

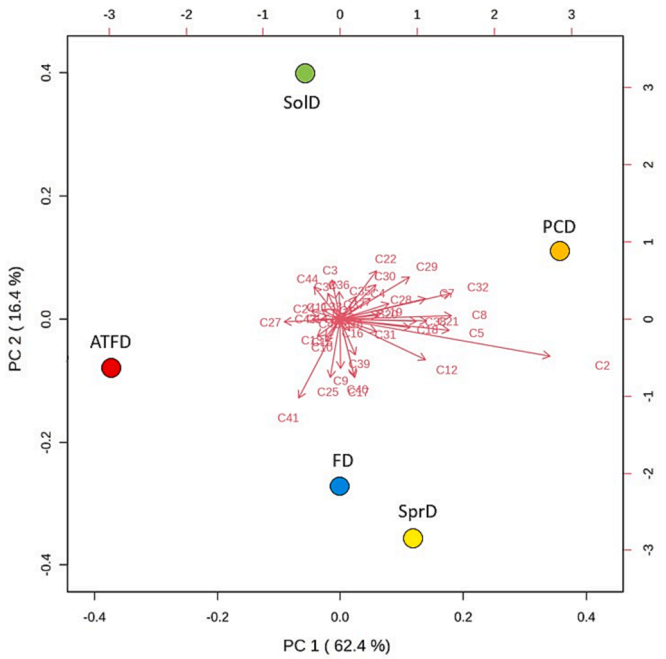

Fig. 6. Distribution of identified VOCs heterotrophic *C. vulgaris* after freeze, spray, agitated thin film, pulse combustion and solar drying, visualized on a PCA scores plot. The first 2 principle components explain 78.8 % of the variance. The VOCs (C) are represented by a red arrow and are listed in the supplementary data. (For interpretation of the references to color in this figure legend, the reader is referred to the web version of this article.)

typical banana-like fruity smell. Dimethyl disulfide and isoamyl acetate, compounds that can be formed during microbial fermentation, suggest microbial activity during solar drying. This is plausible given the 21 h drying time and concurrent temperature range of 25–35 °C, which is optimal for microbial growth.

The correlation between the sensory attributes yeast, cacao and earthy odor with the detected VOCs is presented in a heat plot in Fig. 7. Each VOC typically corresponds to a certain odor, while an odor attribute perceived by smelling may be a mixture of different VOCs. Hence a correlation analysis is performed to better understand how the VOCs are responsible for a certain odor experience. Earthy odor correlated strongest with pentanal (fermented, bready odor), hexanal (grassy), 1-octen-3-ol (earthy, mushroom), 2-heptanone (banana, cheesy) and 2,3-butanedione (buttery). Cacao odor had highest correlation values with 2-methylpropanal (sweet, fruity), 3-methylbutanal (cacao, roasted), methanethiol (cabbage, garlic), 2-methylbutanal (cocoa, malty) and hexanal (grassy). Interestingly, the attribute cacao odor correlates well with Strecker aldehydes that typically provide roasted, sweet, chocolaty odors (Mottram, 2007). Yeast odor correlated strongest with 2-methylpropanal (sweet, fruity), 3-methylbutanal (cacao, fruity), methanethiol (cabbage, garlic), 2-methylbutanal (cocoa, malty) and benzeneacetaldehyde (sweet, almond-like). This result was similar to the correlation of cacao odor, indicating that the panel members had difficulties in distinguishing the two odors.

4. Conclusion

This research shows that the type of drying method influences the techno-functional properties, protein digestibility as well as sensorial properties of *C. vulgaris* single cell proteins. ATFD emerged as a promising drying method that enhanced functional properties of *C. vulgaris* (gelling properties, solubility and water holding properties) as well as the digestibility (N-solubility). We hypothesized that these effects could be attributed to the phenomenon of cell disruption, likely due to the higher drying temperature (98 °C) for a prolonged period of time (10 min) combined with mechanical forces rupturing the *C. vulgaris* cell wall. Furthermore, substantial protein denaturation was detected in the ATFD powder which likely further contributed to these properties. In contrast, the other four drying techniques did not result in substantial differences in *C. vulgaris* protein quality. In general, dried heterotrophic *C. vulgaris* is characterized by competitive lipid-related techno-functional properties such as emulsifying and lipid-binding properties compared the commercial SI and EWI. Nonetheless, the microalgal single cell protein shows room for improvement with other functional properties as well as digestibility. The sensory evaluation indicated formation of an earthy off-odor after ATFD. This correlated with an increase in the oxidation products 1-octen-3-ol, pentanal and hexanal suggesting fatty acid oxidation during drying possibly due to increased cell disruption. High-temperature drying methods such as PCD lead to an increase in cacao odor, which could be linked to an increase in Strecker aldehydes and furans. This study demonstrates that, depending on the application of the microalgal powder, a reasoned choice should be made on the selection of the drying technique. Although cost is a major incentive for producers, some applications require highly functional properties, high digestibility or a specific flavor profile that could be obtained by applying a certain drying method. Cell disruption and drying are both energy intensive processes, which makes ATFD an interesting technique to potentially achieve both steps with lower total energy costs. In respect to energy, FD and SprD are known for their high electricity usage. Techniques such as PCD have energetically improved the SprD process, but suffer from the need to burn fossil fuels (Zbicinski, 2002). On the other hand, ATFD is generally characterized by high thermal efficiency with lower energy consumption while SolD reduces the need for electricity by applying solar thermal energy, resulting in lower overall drying costs (Acar et al., 2022; López Pastor, Pinna-Hernández, & Acién Fernández, 2023). These findings can contribute to the development of a tailored approach to different microalgae single cell protein use-cases. Future research should focus on more effective cell disruption techniques and/or protein purification techniques to elucidate the effect of *C. vulgaris* solubilized/purified proteins on functional properties as well as protein digestibility.

Funding

This project has received funding from the European Union's Horizon 2020 research and innovation program under grant agreement No 862,980.

CRediT authorship contribution statement

Simon Van De Walle: Writing – review & editing, Writing – original draft, Visualization, Validation, Project administration, Methodology, Investigation, Formal analysis, Data curation, Conceptualization. **Imma Gifuni:** Writing – review & editing, Project administration, Methodology, Funding acquisition, Data curation, Conceptualization. **Bert Coleman:** Writing – review & editing, Methodology, Formal analysis, Data curation. **Marie-Christin Baune:** . **Alexandre Rodrigues:** . **Helena Cardoso:** . **Fabio Fanari:** . **Koenraad Muylaert:** Writing – review & editing, Supervision, Data curation, Conceptualization. **Geert Van Royen:** Writing – review & editing, Supervision, Project administration, Methodology, Funding acquisition, Data curation, Conceptualization.

Declaration of competing interest

The authors declare that they have no known competing financial interests or personal relationships that could have appeared to influence the work reported in this paper.

Data availability

The data that support the findings of this study are available from the

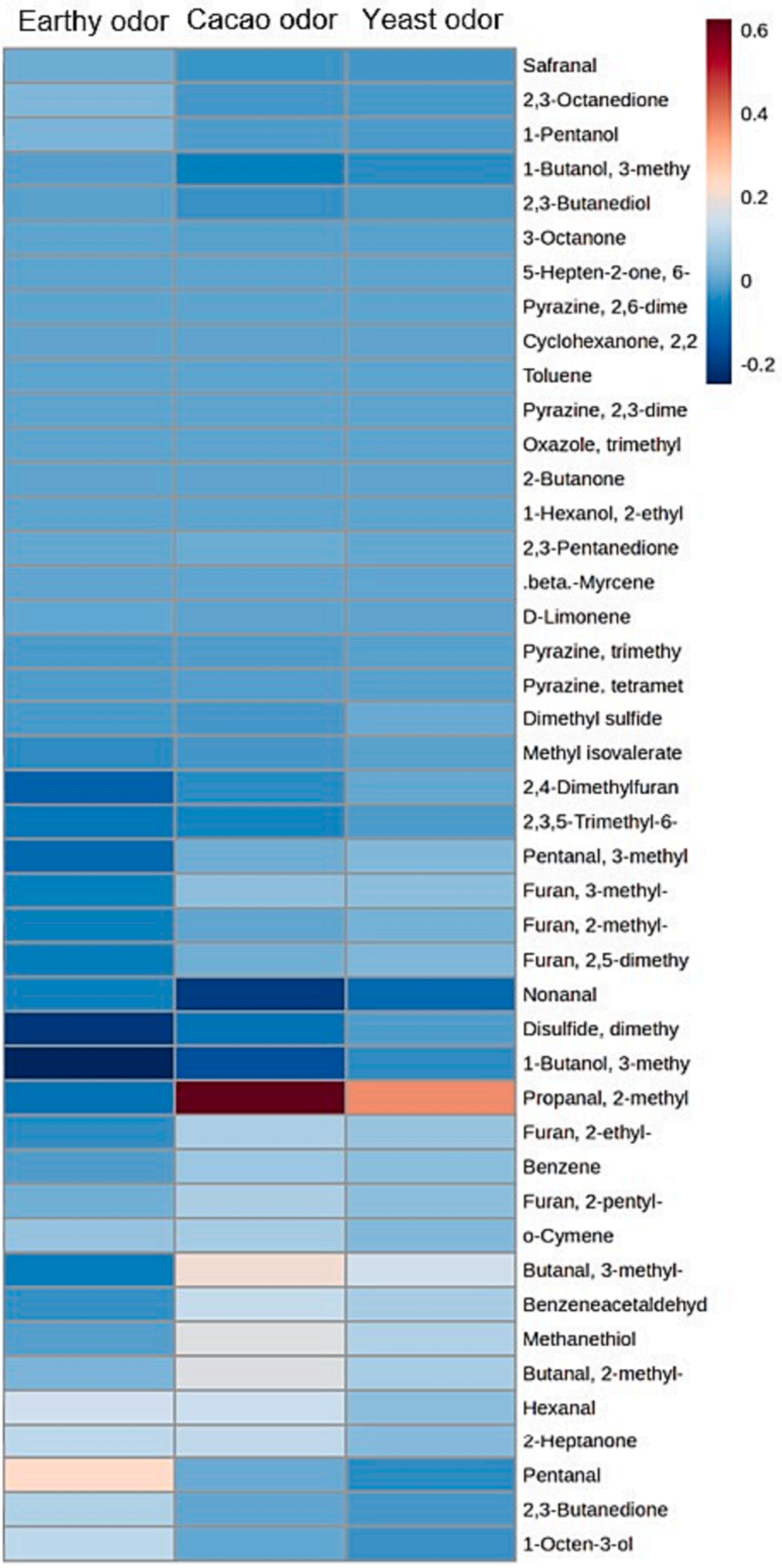

Fig. 7. Heat map representation of correlation coefficients obtained by PLSR analysis between VOCs and the cacao, earthy and yeast odor attributes. High correlations are white to red in color while low correlations are represented in blue. (For interpretation of the references to color in this figure legend, the reader is referred to the web version of this article.)

corresponding author upon reasonable request.

Acknowledgements

The authors would like to thank Benjamin Schmid, Xavier Felipe and Pedro Quelhas for their technical assistance with the drying experiments and optimization of the drying equipment. Thanks to Valentina Casciaro for experimental work on the volatile compound characterization. Thanks to Jana Szkudlarksi for her technical assistance with the techno-functional properties determinations.

Appendix A. Supplementary material

Supplementary data to this article can be found online at https://doi.org/10.1016/j.foodres.2024.114142.

References

Acar, C., Dincer, I., & Mujumdar, A. (2022). A comprehensive review of recent advances in renewable-based drying technologies for a sustainable future. *Drying Technology, 40*(6), 1029–1050. https://doi.org/10.1080/07373937.2020.1848858

Acquah, C., Ekezie, F.-G., & Udenigwe, C. C. (2021). In *Potential applications of microalgae-derived proteins and peptides in the food industry* (pp. 97–126). Elsevier. https://doi.org/10.1016/B978-0-12-821080-2.00011-3.

Adler-Nissen, J. (1979). Determination of the degree of hydrolysis of food protein hydrolysates by trinitrobenzenesulfonic acid. *Journal of Agricultural and Food Chemistry, 27*(6), 1256–1262. https://doi.org/10.1021/jf60226a042

Azmi, A. A. bin, Sankaran, R., Show, P. L., Ling, T. C., Tao, Y., Munawaroh, H. S. H., Kong, P. S., Lee, D. J., & Chang, J. S. (2020). Current application of electrical pre-treatment for enhanced microalgal biomolecules extraction. In *Bioresource Technology* (Vol. 302, p. 122874). Elsevier Ltd. https://doi.org/10.1016/j.biortech.2020.122874.

Barros, A., Pereira, H., Campos, J., Marques, A., Varela, J., & Silva, J. (2019). Heterotrophy as a tool to overcome the long and costly autotrophic scale-up process for large scale production of microalgae. *Scientific Reports, 9*(1). https://doi.org/10.1038/s41598-019-50206-z

Batista, S., Pintado, M., Marques, A., Abreu, H., Silva, J. L., Jessen, F., Tulli, F., & Valente, L. M. P. (2020). Use of technological processing of seaweed and microalgae as strategy to improve their apparent digestibility coefficients in European seabass (Dicentrarchus labrax) juveniles. *Journal of Applied Phycology, 32*(5), 3429–3446. https://doi.org/10.1007/S10811-020-02185-2/TABLES/9

Benelhadj, S., Gharsallaoui, A., Degraeve, P., Attia, H., & Ghorbel, D. (2016). Effect of pH on the functional properties of Arthrospira (Spirulina) platensis protein isolate. *Food Chemistry, 194*, 1056–1063. https://doi.org/10.1016/j.foodchem.2015.08.133

Bertsch, P., Böcker, L., Mathys, A., & Fischer, P. (2021). Proteins from microalgae for the stabilization of fluid interfaces, emulsions, and foams. *Trends in Food Science and Technology*, *108*(December 2020), 326–342. https://doi.org/10.1016/j.tifs.2020.12.014.

Birch, A. N., Petersen, M. A., Arneborg, N., & Hansen, Å. S. (2013). *Influence of commercial baker's yeasts on bread aroma profiles.*. https://doi.org/10.1016/j.foodres.2013.03.011

Brodkorb, A., Croguennec, T., Bouhallab, S., & Kehoe, J. J. (2016). Heat-induced denaturation, aggregation and gelation of whey proteins. *Advanced Dairy Chemistry: Volume 1B: Proteins: Applied Aspects: Fourth Edition*, 155–178. https://doi.org/10.1007/978-1-4939-2800-2_6/FIGURES/7

Brodkorb, A., Egger, L., Alminger, M., Alvito, P., Assunção, R., Ballance, S., … Recio, I. (2019). INFOGEST static in vitro simulation of gastrointestinal food digestion. *Nature Protocols, 14*(4), 991–1014. https://doi.org/10.1038/s41596-018-0119-1

Broucke, K., Van Poucke, C., Duquenne, B., De Witte, B., Baune, M. C., Lammers, V., Terjung, N., Ebert, S., Gibis, M., Weiss, J., & Van Royen, G. (2022). Ability of (extruded) pea protein products to partially replace pork meat in emulsified cooked sausages. *Innovative Food Science and Emerging Technologies, 78*(April), Article 102992. https://doi.org/10.1016/j.ifset.2022.102992

Calderón-Castro, A., Jacobo-Valenzuela, N., Félix-Salazar, L. A., de Zazueta-Morales, J., Martínez-Bustos, F., Fitch-Vargas, P. R., Carrillo-López, A., & Aguilar-Palazuelos, E. (2019). Optimization of corn starch acetylation and succinylation using the extrusion process. *Journal of Food Science and Technology, 56*(8), 3940–3950. https://doi.org/10.1007/s13197-019-03863-x

Canelli, G., Murciano Martínez, P., Austin, S., Ambü Hl, M. E., Dionisi, F., Bolten, C. J., Carpine, R., Neutsch, L., & Mathys, A. (2021). Biochemical and morphological characterization of heterotrophic *Crypthecodinium cohnii* and chlorella vulgaris cell walls. *Cite This: J. Agric. Food Chem, 69*. https://doi.org/10.1021/acs.jafc.0c05032

Carullo, D., Abera, B. D., Casazza, A. A., Donsì, F., Perego, P., Ferrari, G., & Pataro, G. (2018). Effect of pulsed electric fields and high pressure homogenization on the aqueous extraction of intracellular compounds from the microalgae Chlorella vulgaris. *Algal Research, 31*, 60–69. https://doi.org/10.1016/j.algal.2018.01.017

Chen, C. L., Chang, J. S., & Lee, D. J. (2015). Dewatering and drying methods for microalgae. *Drying Technology, 33*(4), 443–454. https://doi.org/10.1080/07373937.2014.997881

Clavijo Rivera, E., Montalescot, V., Viau, M., Drouin, D., Bourseau, P., Frappart, M., Monteux, C., & Couallier, E. (2018). Mechanical cell disruption of Parachlorella kessleri microalgae: Impact on lipid fraction composition. *Bioresource Technology, 256*, 77–85. https://doi.org/10.1016/j.biortech.2018.01.148

Coleman, B. (2023). *The potential of microalgae as flavoring agent for plant-based seafood alternatives*. KU Leuven.

Coleman, B., Van Poucke, C., De Witte, B., Casciaro, V., Moerdijk-Poortvliet, T., Muylaert, K., & Robbens, J. (2023). The effect of drying, cell disruption and storage on the sensory properties of Nannochloropsis sp. *Algal Research, 71*, Article 103092. https://doi.org/10.1016/j.algal.2023.103092

Coleman, B., Van Poucke, C., Dewitte, B., Ruttens, A., Moerdijk-Poortvliet, T., Latsos, C., De Reu, K., Blommaert, L., Duquenne, B., Timmermans, K., van Houcke, J., Muylaert, K., & Robbens, J. (2022). Potential of microalgae as flavoring agents for plant-based seafood alternatives. *Future Foods, 5*. https://doi.org/10.1016/j.fufo.2022.100139

Crews, C., & Castle, L. (2007). A review of the occurrence, formation and analysis of furan in heat-processed foods. *Trends in Food Science and Technology, 18*(7), 365–372. https://doi.org/10.1016/j.tifs.2007.03.006

Dai, L., Cepeda, M., Hinrichs, J., & Weiss, J. (2021). Behavior of concentrated emulsions prepared by acid-hydrolyzed insoluble microalgae proteins from Chlorella protothecoides. *Journal of the Science of Food and Agriculture, 101*(8), 3348–3354. https://doi.org/10.1002/JSFA.10964

de Farias Neves, F., Demarco, M., & Tribuzi, G. (2020). Drying and quality of microalgal powders for human alimentation. In *Microalgae - From physiology to application*. IntechOpen. https://doi.org/10.5772/intechopen.89324.

Demarco, M., Oliveira de Moraes, J., Matos, Â. P., Derner, R. B., de Farias Neves, F., & Tribuzi, G. (2022). Digestibility, bioaccessibility and bioactivity of compounds from algae. *Trends in Food Science & Technology*, *121*(October 2021), 114–128. https://doi.org/10.1016/j.tifs.2022.02.004.

Dubois, M., Gilles, K. A., Hamilton, J. K., Rebers, P. A., & Smith, F. (1956). Colorimetric method for determination of sugars and related substances. *Analytical Chemistry, 28*(3), 350–356. https://doi.org/10.1021/AC60111A017/ASSET/AC60111A017.FP.PNG_V03

Ebert, S., Grossmann, L., Hinrichs, J., & Weiss, J. (2019). Emulsifying properties of water-soluble proteins extracted from the microalgae: Chlorella sorokiniana and Phaeodactylum tricornutum. *Food and Function, 10*(2), 754–764. https://doi.org/10.1039/c8fo02197j

Freeman, H. J., Kim, Y. S., & Sleisenger, M. H. (1979). Protein digestion and absorption in man: Normal mechanisms and protein-energy malnutrition. *The American Journal of Medicine, 67*(6), 1030–1036. https://doi.org/10.1016/0002-9343(79)90645-4

Geada, P., Moreira, C., Silva, M., Nunes, R., Madureira, L., Rocha, C. M. R., Pereira, R. N., Vicente, A. A., & Teixeira, J. A. (2021). Algal proteins: Production strategies and nutritional and functional properties. In *Bioresource Technology* (Vol. 332, p. 125125). Elsevier Ltd. https://doi.org/10.1016/j.biortech.2021.125125.

Grossmann, L., Ebert, S., Rg Hinrichs, J., & Weiss, J. (2019). *Formation and Stability of Emulsions Prepared with a Water-Soluble Extract from the Microalga Chlorella protothecoides*. https://doi.org/10.1021/acs.jafc.8b05337

Grossmann, L., Wörner, V., Hinrichs, J., & Weiss, J. (2020). Sensory properties of aqueous dispersions of protein-rich extracts from Chlorella protothecoides at neutral and acidic pH. In *Journal of the Science of Food and Agriculture* (Vol. 100, Issue 3, pp. 1344–1349). https://doi.org/10.1002/jsfa.10082.

Guil-Guerrero, J. L., Navarro-Juárez, R., López-Martínez, J. C., Campra-Madrid, P., & Rebolloso-Fuentes, M. M. (2004). Functional properties of the biomass of three microalgal species. *Journal of Food Engineering, 65*(4), 511–517. https://doi.org/10.1016/j.jfoodeng.2004.02.014

Kim, H. S., Park, W. K., Lee, B., Seon, G., Suh, W. I., Moon, M., & Chang, Y. K. (2019). Optimization of heterotrophic cultivation of Chlorella sp. HS2 using screening, statistical assessment, and validation. In *Scientific Reports* (Vol. 9, Issue 1). https://doi.org/10.1038/s41598-019-55854-9.

Klamczynska, B., & Mooney, W. D. (2017). Heterotrophic microalgae: A scalable and sustainable protein source. In *Sustainable Protein Sources* (pp. 327–339). https://doi.org/10.1016/B978-0-12-802778-3.00020-2.

Lam, R. S. H., & Nickerson, M. T. (2013). Food proteins: A review on their emulsifying properties using a structure-function approach. *Food Chemistry, 141*(2), 975–984. https://doi.org/10.1016/j.foodchem.2013.04.038

Lenth, R. V. (2016). Least-squares means: The R package {lsmeans}. *Journal of Statistical Software, 69*(1), 1–33. https://doi.org/10.18637/jss.v069.i01.

Liland, K. H., Mevik, B.-H., & Wehrens, R. (2022). *pls: Partial least squares and principal component regression*. https://cran.r-project.org/package=pls.

López Pastor, R., Pinna-Hernández, M. G., & Acién Fernández, F. G. (2023). Technical and economic viability of using solar thermal energy for microalgae drying. In *Energy Reports* (Vol. 10, pp. 989–1003). https://doi.org/10.1016/j.egyr.2023.07.040.

Lourenço, S. O., Barbarino, E., Lavín, P. L., Lanfer Marquez, U. M., & Aidar, E. (2004). Distribution of intracellular nitrogen in marine microalgae: Calculation of new nitrogen-to-protein conversion factors. *European Journal of Phycology, 39*(1), 17–32. https://doi.org/10.1080/0967026032000157156

Lupatini Menegotto, A. L., de Souza, L. E. S., Colla, L. M., Costa, J. A. V., Sehn, E., Bittencourt, P. R. S., de Moraes Flores, É. L., Canan, C., & Colla, E. (2019). Investigation of techno-functional and physicochemical properties of Spirulina platensis protein concentrate for food enrichment. *Lwt, 114*. https://doi.org/10.1016/j.lwt.2019.108267

Minekus, M., Alminger, M., Alvito, P., Ballance, S., Bohn, T., Bourlieu, C., … Brodkorb, A. (2014). A standardised static in vitro digestion method suitable for food-an international consensus. *Food and Function, 5*(6), 1113–1124. https://doi.org/10.1039/c3fo60702j

Mottram, D. S. (2007). The maillard reaction: Source of flavour in thermally processed foods. *Flavours and Fragrances: Chemistry, Bioprocessing and Sustainability, 269–283*. https://doi.org/10.1007/978-3-540-49339-6_12/COVER

Qiu, J., Boom, R. M., & Schutyser, M. A. I. (2019). Agitated thin-film drying of foods. *Drying Technology, 37*(6), 735–744. https://doi.org/10.1080/07373937.2018.1458037

R Core Team. (2020). A Language and environment for statistical computing. In *R Foundation for Statistical Computing* (p. https://www.R-project.org). http://www.r-project.org.

Rattanapoltee, P., & Kaewkannetra, P. (2014). *Cultivation of microalga, Chlorella vulgaris under different autoeheteroemixo trophic growths as a raw material during biodiesel production and cost evaluation.* https://doi.org/10.1016/j.energy.2014.06.049

Rieder, A., Afseth, N. K., Böcker, U., Knutsen, S. H., Kirkhus, B., Mæhre, H. K., Ballance, S., & Wubshet, S. G. (2021). Improved estimation of in vitro protein digestibility of different foods using size exclusion chromatography. *Food Chemistry, 358*(November 2020). https://doi.org/10.1016/j.foodchem.2021.129830

Saha, D., & Bhattacharya, S. (2010). Hydrocolloids as thickening and gelling agents in food: A critical review. *Journal of Food Science and Technology, 47*(6), 587–597. https://doi.org/10.1007/s13197-010-0162-6

Samborska, K., Poozesh, S., Baránskabaránska, A., Sobulska, M., Jedlínskajedlínska, A., Arpagaus, C., Malekjani, N., & Jafari, S. M. (2022). Innovations in spray drying process for food and pharma industries. *Journal of Food Engineering, 321*, Article 110960. https://doi.org/10.1016/j.jfoodeng.2022.110960

Schmid, B., Navalho, S., Schulze, P. S. C., Van De Walle, S., De, V., Van Van Royen, G., Schüler, L. M., Maia, I. B., Bastos, C. R. V., Baune, M.-C., Januschewski, E., Coelho, A., Pereira, H., Varela, J., Navalho, J., & Cavaco Rodrigues, A. M. C. (2022). Drying microalgae using an industrial solar dryer: A biomass quality assessment. *Foods, 11*(13), 1873. https://doi.org/10.3390/FOODS11131873

Schüler, L., Greque de Morais, E., Trovão, M., Machado, A., Carvalho, B., Carneiro, M., Maia, I., Soares, M., Duarte, P., Barros, A., Pereira, H., Silva, J., & Varela, J. (2020). Isolation and characterization of novel chlorella vulgaris mutants with low chlorophyll and improved protein contents for food applications. *Frontiers in Bioengineering and Biotechnology, 8*(May), 1–10. https://doi.org/10.3389/fbioe.2020.00469

Shkolnikov Lozober, H., Okun, Z., & Shpigelman, A. (2021). The impact of high-pressure homogenization on thermal gelation of Arthrospira platensis (Spirulina) protein concentrate. In *Innovative Food Science & Emerging Technologies* (Vol. 74, p. 102857). https://doi.org/10.1016/j.ifset.2021.102857.

Show, K. Y., Lee, D. J., Tay, J. H., Lee, T. M., & Chang, J. S. (2015). Microalgal drying and cell disruption – Recent advances. *Bioresource Technology, 184*, 258–266. https://doi.org/10.1016/J.BIORTECH.2014.10.139

Soto-Sierra, L., Stoykova, P., & Nikolov, Z. L. (2018). Extraction and fractionation of microalgae-based protein products. In *Algal Research* (Vol. 36, pp. 175–192). Elsevier B.V. https://doi.org/10.1016/j.algal.2018.10.023.

Stone, A. K., Karalash, A., Tyler, R. T., Warkentin, T. D., & Nickerson, M. T. (2015). Functional attributes of pea protein isolates prepared using different extraction methods and cultivars. In *Food Research International* (Vol. 76, Issue P1, pp. 31–38). https://doi.org/10.1016/j.foodres.2014.11.017.

Stramarkou, M., Papadaki, S., Kyriakopoulou, K., & Krokida, M. (2017). Effect of drying and extraction conditions on the recovery of bioactive compounds from Chlorella vulgaris. *Journal of Applied Phycology, 29*(6), 2947–2960. https://doi.org/10.1007/s10811-017-1181-8

Sun, X. D., & Arntfield, S. D. (2010). Gelation properties of salt-extracted pea protein induced by heat treatment. *Food Research International, 43*(2), 509–515. https://doi.org/10.1016/j.foodres.2009.09.039

Teuling, E., Schrama, J. W., Gruppen, H., & Wierenga, P. A. (2017). Effect of cell wall characteristics on algae nutrient digestibility in Nile tilapia (Oreochromis niloticus) and African catfish (Clarus gariepinus). *Aquaculture, 479*, 490–500. https://doi.org/10.1016/J.AQUACULTURE.2017.06.025

Van De Walle, S., Broucke, K., Baune, M.-C., Terjung, N., Van Royen, G., & Boukid, F. (2023). Microalgae protein digestibility: How to crack open the black box? 1–23. https://doi.org/10.1080/10408398.2023.2181754.

Vera Zambrano, M., Dutta, B., Mercer, D. G., MacLean, H. L., & Touchie, M. F. (2019). Assessment of moisture content measurement methods of dried food products in small-scale operations in developing countries: A review. In *Trends in Food Science and Technology* (Vol. 88, pp. 484–496). https://doi.org/10.1016/j.tifs.2019.04.006.

Verfaillie, D., Janssen, F., Van Royen, G., & Wouters, A. G. B. (2023). A systematic study of the impact of the isoelectric precipitation process on the physical properties and protein composition of soy protein isolates. *Food Research International, 163*, Article 112177. https://doi.org/10.1016/j.foodres.2022.112177

Wijayanti, H. B., Brodkorb, A., Hogan, S. A., & Murphy, E. G. (2019). *Thermal denaturation, aggregation, and methods of Prevention.* https://doi.org/10.1016/B978-0-12-812124-5.00006-0

Xiong, T., Xiong, W., Ge, M., Xia, J., Li, B., & Chen, Y. (2018). Effect of high intensity ultrasound on structure and foaming properties of pea protein isolate. In *Food Research International* (Vol. 109, pp. 260–267). https://doi.org/10.1016/j.foodres.2018.04.044.

Yin, S. W., Tang, C. H., Wen, Q. B., Yang, X. Q., & Li, L. (2008). Functional properties and in vitro trypsin digestibility of red kidney bean (Phaseolus vulgaris L.) protein isolate: Effect of high-pressure treatment. *Food Chemistry, 110*(4), 938–945. https://doi.org/10.1016/J.FOODCHEM.2008.02.090

Zayas, J. F. (1997). Functionality of proteins in food. In *Functionality of proteins in food*. Berlin Heidelberg: Springer. https://doi.org/10.1007/978-3-642-59116-7.

Zbicinski, I. (2002). Equipment, technology, perspectives and modeling of pulse combustion drying. *Chemical Engineering Journal, 86*, 33–46. https://doi.org/10.1016/S1385-8947(01)00269-8

Zhang, H., Gong, T., Li, J., Pan, B., Hu, Q., Duan, M., & Zhang, X. (2022). Study on the effect of spray drying process on the quality of microalgal biomass: A comprehensive biocomposition analysis of spray-dried *S. acuminatus* biomass. *Bioenergy Research, 15*(1), 320–333. https://doi.org/10.1007/S12155-021-10343-8/FIGURES/5

Zheng, T., Li, X., Taha, A., Wei, Y., Hu, T., Fatamorgana, P. B., Zhang, Z., Liu, F., Xu, X., Pan, S., & Hu, H. (2019). Effect of high intensity ultrasound on the structure and physicochemical properties of soy protein isolates produced by different denaturation methods. *Food Hydrocolloids, 97*, Article 105216. https://doi.org/10.1016/J.FOODHYD.2019.105216